Slow algebraic relaxation in quartic potentials and related results

Robert S. Sinkovits
San Diego Supercomputer Center, San Diego, California 92186-5608

Surajit Sen*
Department of Physics and Center for Advanced Photonic and Electronic Materials, State University of New York at Buffalo, Buffalo, New York 14260-1500

James Christopher Phillips
Department of Physics and Beckman Institute, University of Illinois at Urbana–Champaign, Urbana, Illinois 61801

Soumya Chakravarti
Department of Physics, California State Polytechnic University, Pomona, California 91768
(Received 2 June 1998)

We present a detailed report [see S. Sen *et al.*, Phys. Rev. Lett. **77**, 4855 (1996)] of our *numerical* and *analytical* studies on the relaxation of a classical particle in the potentials $V(x)=\pm x^2/2+x^4/4$. Both of the approaches confirm that at all temperatures, the relaxation functions (e.g., velocity relaxation function and position relaxation function) decay asymptotically in time t as $\sin(\omega_0 t)/t$. Numerically calculated power spectra of the relaxation functions show a gradual transition with increasing temperature from a single sharp peak located at the harmonic frequency ω_0 to a broad continuous band. The $1/t$ relaxation is also found when $V(x)$ is a polynomial in powers of x^2 with a nonvanishing coefficient accompanying the x^4 term in $V(x)$. Numerical calculations show that in the cases in which the leading term in $V(x)$ behaves as x^{2n} with integer n, the asymptotic relaxation exhibits $1/t^{\phi}$ decay where $\phi=1/(n-1)$. We briefly discuss the analytical approaches to relaxation studies in these strongly anharmonic systems using direct solution of the equation of motion and using the continued fraction formalism approach for relaxation studies. We show that the study of the dynamics of strongly anharmonic oscillators poses unique difficulties when studied via the continued fraction or any other time-series construction based approaches. We close with comments on the physical processes in which the insights presented in this work may be applicable. [S1063-651X(99)09306-X]

PACS number(s): 67.40.Fd, 65.90.+i

I. INTRODUCTION

There is a close connection between the behavior of a classical particle relaxing in an anharmonic multiwell potential at a fixed temperature and a number of more complex physical phenomena such as the dynamical processes associated with structural phase transitions [1] and with relaxation processes in glassy systems [2,3]. An important illustrative example is that of the Krumhansl-Schrieffer (KS) model, which is a simplistic model for displacive structural phase transitions [1]. The KS-type model can be described by a Hamiltonian $H=\Sigma_i(H_i+H_{i,i+1})$, where H_i and $H_{i,i+1}$ are of the following forms:

$$H_i=\frac{1}{2}m\dot{x}_i^2+\frac{A_i x_i^2}{2}+\frac{B_i x_i^{2n_i}}{2n_i}+C_i\Gamma_i(x_i^{\mu_i};\mu_i>2n_i) \quad (1)$$

and

$$H_{i,i+1}=\frac{k_{i,i+1}}{2}(x_i-x_{i+1})^2, \quad (2)$$

where $\dot{x}_i, x_i$ denote the velocity and the position of some ith particle of mass m, $B_i>0$, $k_{i,i+1}$ denotes the spring constants of the springs connecting the nearest-neighbor masses, and Γ_i is an unspecified anharmonic piece in the one-body potential landscape which, in general, involves terms of $O(x^{2n_i+2})$ or higher. We note that $n_i \geqslant 1$ and is an integer. Thus, by appropriate choice of Γ_i one can construct a one-body potential which can be a cosh, cos, exp, or some other function. A_i, B_i, C_i are real coupling constants which determine the potential energy landscape of particle i. A_i can be positive or negative. Let us assume that as the total energy of the system, $E\to 0$, each particle finds itself in a bounded potential. From now on, for the sake of simplicity, let us also suppose that $k_{i,i+1}=k$.

If we set $A_i=B_i=C_i=0$ in Eq. (1), then the dynamical problem for the Hamiltonian H can be analytically solved for all N including in the limit $N\to\infty$. It has been shown by Fox [4], Florencio and Lee [5], Vitali and Grigolini [6], and others that in the thermodynamic limit, i.e., as $N\to\infty$, the normalized velocity autocorrelation function of any particle (say j), $\langle v_j(t)v_j(0)\rangle/\langle v_j(0)^2\rangle=(k_BT/m)J_0(\omega_0 t)$, $\omega_0=\sqrt{k/m}$, where $J_0(\omega_0 t)$ is a zeroth-order Bessel function which decays in time in an oscillatory algebraic manner, k_B is the Boltzmann constant. The decay exponent here behaves as $t^{-3/2}$ [4–6]. This behavior is robust for the other dynamical

*Author to whom correspondence should be addressed.

correlations, such as the position and acceleration autocorrelations, of the harmonic-oscillator chain as well [5].

As we shall demonstrate below, if $k=0$ and $A_i \neq 0$, $B_i > 0$, the asymptotic relaxation of any corresponding autocorrelation function turns out to be *significantly slower* than $t^{-3/2}$. We will not discuss the consequences of the terms with coefficients C_i in this work except to say that our numerical analyses reported in [7] reveal that the asymptotic relaxation of a single classical particle in an anharmonic potential is controlled by the leading anharmonic term and *not* by the higher-order terms in a potential such as that described by Eq. (1).

If $k \ll |A_i|$, $k \ll B_i$, then it is not unreasonable to expect that there would be a distinct separation of relaxation mechanisms arising from the noninteracting and the interacting parts of the Hamiltonian. The slower relaxation, arising from the anharmonic interactions, could presumably dominate as $t \to \infty$. An intuitive argument in favor of the case that the slower one-body relaxation may win out as time $t \to \infty$ comes from noting that coupling oscillators via nearest-neighbor harmonic springs in a locally anharmonic potential with leading anharmonicity of form x^{2n} will not effectively further stiffen the local x^{2n} anharmonicity. The argument is expected to be quite robust at low temperatures in which the amplitudes of motion of the particles are small and are dominated by the acoustic mode, i.e., in the so-called ''order-disorder'' regime [1,8]. Since there is no phase transition for models such as in Eqs. (1) and (2) in one dimension, the above-mentioned argument, namely that the long time relaxation will be dictated by local anharmonicities, may even hold at all finite temperatures. Difficulties could arise, however, if the two-body interaction becomes strongly anharmonic such that the local anharmonicity will be strongly affected by the two-body interaction. We shall return to a more technical discussion of the connections between the one-body and the many-body relaxations later in Secs. VII and VIII in this paper.

A detailed understanding of relaxation in one-dimensional (1D) multiwell potentials could lead to greater insights into the dynamics of not only the KS model but in models of thermally activated dynamics in the glass transition and of relaxation in related complex systems.

In a recent Letter [7], we have presented results which show that the relaxation of a classical particle in anharmonic potentials follows a power law which depends upon the order of the leading anharmonic term. For potentials with a leading quartic anharmonicity, the relaxation functions show a $1/t$ decay. In the present paper, we first present a detailed discussion of the behavior of a particle relaxing in the potentials $V(x) = \pm x^2/2 + x^4/4$. Choosing the ''+'' sign in this potential results in a single symmetric well with a minimum at $x = 0$, while choosing the ''−'' sign leads to a symmetric double well with minima at $x = \pm 1$. Throughout the remainder of this paper, for the sake of clarity we will refer to the first case as the Duffing well and to the second case as the double well, respectively, although the so-called double-well case is one realization of the case of the Duffing well [9]. We refer the reader to our study in [7] for a discussion and for results on relaxation in potentials that differ from the Duffing and double wells but possess leading quartic anharmonicity. In particular, we briefly discuss relaxation processes in cases $V(x) = \cosh(x)$ and $V(x) = \cos(x)$ in Ref. [7]. As we shall see, in all of these cases, the relaxation function decays asymptotically in time as $1/t$. We then present a brief discussion of relaxation in which the leading anharmonicity in the potential is of the form x^{2n}, where $n > 2$, where one encounters asymptotic relaxation of the form $1/t^{\phi}$, where $\phi = 1/(n-1)$. We then apply this result to discuss the special cases of $n = 1$ and $n \to \infty$. It is possible to prove this result, which was initially arrived at using numerical methods, via some limiting analyses as done by Sarkar [10]. It should be noted, however, that Sarkar's [10] or any existing analyses [11] do not solve the dynamical problem as a function of time, but rather succeed in obtaining the behavior of the lowest frequency of the anharmonic oscillator as a functon of total energy to leading order in energy. A powerful analytical tool for studying relaxation phenomena relies upon the continued fraction formalism (CFF) [12–17]. While a large class of systems can be readily probed using the CFF, it turns out that one encounters grave difficulties in implementing the CFF in studying relaxation processes in strongly anharmonic oscillators [18,19]. In closing, we discuss these difficulties, we summarize our numerical and analytical work, and discuss its implications.

We begin by presenting the derivation of the asymptotic $1/t$ behavior of the relaxation function starting from the formal solution of the Duffing oscillator in Sec. II A. The extension of the asymptotic relaxation analyses to cases with leading anharmonicity of the form x^{2n}, where $n > 2$, is presented in Sec. II B. We then go on to describe in some detail the numerical method employed in calculating the relaxation functions in Sec. III. The studies on relaxation processes in other potentials with leading quartic and with leading higher-order anharmonicities are presented in Secs. IV and V, respectively. The analytical approach to studying relaxation processes in anharmonic oscillators, such as the continued fraction formalism (CFF), presents a unique set of problems in getting to the correct answers. These issues are discussed in Sec. VI. The applications of these results to many-body systems of interest in condensed matter and statistical physics are presented in Sec. VII. We summarize the work and present open questions of broad interest in the analyses of slow relaxation problems in Sec. VIII.

II. ANALYTIC BEHAVIOR

A. Quartic anharmonicity: Duffing and double wells

In this section we derive analytic results for the behavior of the canonical velocity autocorrelation function in the limit $t \to \infty$. We use the formal solution of the Duffing potential $V(x) = x^2/2 + rx^4/4$, $r > 0$, as the starting point for the derivation. We do not work out the case for the double well explicitly but refer the interested reader to the treatment of Davis [9] for working out the minor modifications in the formulae in Eqs. (3)–(8) and (12) below. We shall argue that the asymptotic relaxation properties of a particle in the Duffing and double wells are identical.

The location of a particle with a fixed energy moving in the Duffing potential is given by

$$x(t) = C \sum_{p=0}^{\infty} a_p \sin(2p+1)\omega t, \tag{3}$$

where the leading terms of the constants Ca_p are

$$Ca_0 = a, \tag{4}$$

$$Ca_1 = (-ra^3/32)(1 - 21ra^2/32 + 461r^2a^4/1024 + \cdots), \tag{5}$$

$$Ca_2 = (r^2a^5/1024)(1 - 43ra^2/32 + \cdots), \ldots, \tag{6}$$

and the frequency ω is

$$\omega = (1 + 3ra^2/4 + 3r^2a^4/128 - 57r^3a^6/4096 + \cdots)^{1/2}. \tag{7}$$

In the above expressions, the variable a is obtained as a function of E by substituting the formal solutions for $x(t)$ and $v(t)$ into the Hamiltonian $p^2/2m + V$, where $m = 1$, yielding

$$a = (2E)^{1/2} - \frac{9E^{3/2}}{2^{7/2}} + \frac{561E^{5/2}}{2^{17/2}} \cdots. \tag{8}$$

The normalized microcanonical ensemble velocity autocorrelation function (VACF) is obtained by substituting $dx(t)/dt$ into the equation

$$\frac{\langle v(0)v(t)\rangle_E}{\langle v(0)^2\rangle_E} = \frac{\int_{-\infty}^{\infty} v(t')v(t'+t)dt'}{\int_{-\infty}^{\infty} v(t')v(t')dt'}, \tag{9}$$

where the subscript E is used to distinguish the microcanonical from the canonical.

The VACF can be greatly simplified by noting that

$$\lim_{t_0 \to \infty} \frac{1}{t_0} \int_{-t_0}^{t_0} \cos(2n+1)\omega t' \cos(2m+1)\omega(t'+t)dt' = \delta_{nm} \cos(2n+1)\omega t, \tag{10}$$

yielding the result

$$\frac{\langle v(0)v(t)\rangle_E}{\langle v(0)^2\rangle_E} = \frac{C^2 \sum_{p=0}^{\infty} a_p^2 (2p+1)^2 \cos(2p+1)\omega t}{C^2 \sum_{p=0}^{\infty} a_p^2 (2p+1)^2}. \tag{11}$$

The above result is an exact form for the microcanonical VACF, but a much simplified form for the canonical VACF can be obtained as follows. One begins by retaining only the lowest-order terms of $\langle v(0)v(t)\rangle_E$ in a. First expanding ω to lowest order in a yields

$$\omega \simeq (1 + 3ra^2/4)^{1/2} \simeq 1 + 3ra^2/8. \tag{12}$$

Substituting this expression into $\langle v(0)v(t)\rangle_E$ and retaining only the $p = 0$ term in the summation gives

$$\frac{\langle v(0)v(t)\rangle_E}{\langle v(0)^2\rangle_E} = \cos(1 + 3ra^2/8)t. \tag{13}$$

Replacing a by its lowest-order expansion in E, setting γ equal to $3r/4$, and substituting the normalized microcanonical VACF into the canonical VACF with the assumption that the density of states $g(E) =$ const at low enough energies (to be elaborated upon in Sec. II B) results in

$$\frac{\langle v(0)v(t)\rangle_{\text{can}}}{\langle v(0)^2\rangle_{\text{can}}} = \frac{\int_0^{\infty} e^{-\beta E} \cos(1 + \gamma E)t dE}{\int_0^{\infty} e^{-\beta E} dE}. \tag{14}$$

Rewriting $\cos(1+\gamma E)t$ as $\cos(t)\cos(\gamma tE) - \sin(t)\sin(\gamma tE)$ and evaluating the integrals

$$\int_0^{\infty} e^{-\beta E} \cos(\gamma tE) dE = \frac{\beta}{\gamma^2 t^2 + \beta^2} \tag{15}$$

and

$$\int_0^{\infty} e^{-\beta E} \sin(\gamma tE) dE = \frac{\gamma t}{\gamma^2 t^2 + \beta^2} \tag{16}$$

results in a form for the low-temperature canonical VACF,

$$\frac{\langle v(0)v(t)\rangle_{\text{can}}}{\langle v(0)^2\rangle_{\text{can}}} = \frac{\beta^2 \cos(t) - \gamma\beta t \sin(t)}{\gamma^2 t^2 + \beta^2}. \tag{17}$$

This form gives an excellent representation of the canonical VACF at all times for $\beta \geqslant 100$ as will be shown in the section on numerical results. In the long-time limit, the expression reduces to

$$\lim_{t \to \infty} \frac{\langle v(0)v(t)\rangle_{\text{can}}}{\langle v(0)^2\rangle_{\text{can}}} = \frac{-(\beta/\gamma)\sin(t)}{t}. \tag{18}$$

Interestingly, this expression describes the long-time behavior of the VACF for all temperatures. This can be shown easily by retaining higher-order terms in E in the expression for the VACF at a fixed energy before substituting into the equation for the canonical VACF. Keeping terms $p > 0$ in the summation leads directly to the appearance of powers of E in the integrals while retaining higher-order terms in the expansion for ω leads to trigonometric functions with arguments involving higher powers of E. This results in contributions to the canonical VACF from integrals of the form

$$\int_0^{\infty} E^p e^{-\beta E} [\cos(\gamma tE), \sin(\gamma tE)] \times [\cos(c_2 tE^2), \sin(c_2 tE^2)] \cdots dE, \tag{19}$$

where the terms in square brackets indicate that one or the other trigonometric function is chosen. Replacing the sin and cos functions containing arguments with powers of E greater than 1 with their series expansions simply results in contributions from a sum of integrals of the form

$$\int_0^{\infty} t^l E^m e^{-\beta E} [\cos(\gamma tE), \sin(\gamma tE)] dE, \tag{20}$$

where all of the powers of E have been collected in E^m, with l and m related by the inequality $m \geqslant l+1$. These integrals have the closed forms

$$I_1 = \int_0^\infty t^l E^m e^{-\beta E} \cos(\gamma t E) dE$$

$$= \frac{t^l m! [(\beta - i\gamma t)^{m+1} + (\beta + i\gamma t)^{m+1}]}{2(\beta^2 + \gamma^2 t^2)^{m+1}} \tag{21}$$

and

$$I_2 = \int_0^\infty t^l E^m e^{-\beta E} \sin(\gamma t E) dE$$

$$= \frac{t^l m! [(\beta - i\gamma t)^{m+1} + (\beta + i\gamma t)^{m+1}]}{2(\beta^2 + \gamma^2 t^2)^{m+1}}. \tag{22}$$

In the long-time limit, the integrals I_1 and I_2 have the behavior

$$\lim_{t\to\infty} I_1 \sim t^{l-m-1}, \quad m \text{ odd}; \quad 0, \quad m \text{ even} \tag{23}$$

and

$$\lim_{t\to\infty} I_2 \sim t^{l-m-1}, \quad m \text{ even}; \quad 0, \quad m \text{ odd}. \tag{24}$$

Since $m-l$ is at least 1, all contributions to the canonical VACF arising from retaining higher-order terms in E decay faster than $1/t$. In the long-time limit, the only surviving term is $-(\beta/\gamma)\sin(t)/t$. We will show in Sec. IV that this asymptotic form does indeed match the numerical simulations at long times for all values of β.

It should be noted that the derivation presented above for the canonical VACF can easily be modified to obtain the canonical autocorrelation functions for other derivatives of $x(t)$. For example, repeating the derivation for $x(t)$ and $a(t)$ would lead to the expressions for the microcanonical autocorrelation functions

$$\frac{\langle x(0)x(t)\rangle_E}{\langle x(0)^2\rangle_E} = \frac{C^2 \sum_{p=0}^{\infty} a_p^2 \cos(2p+1)\omega t}{C^2 \sum_{p=0}^{\infty} a_p^2} \tag{25}$$

and

$$\frac{\langle a(0)a(t)\rangle_E}{\langle a(0)^2\rangle_E} = \frac{C^2 \sum_{p=0}^{\infty} a_p^2 (2p+1)^4 \cos(2p+1)\omega t}{C^2 \sum_{n=0}^{\infty} a_p^2 (2p+1)^4}, \tag{26}$$

respectively. In the limit that only the $p=0$ term in the summation is retained, all of the canonical autocorrelation functions are identical.

For the double well potential, we find that in the limit of low frequency, the frequency of the oscillator is given by $\omega \simeq \sqrt{2} - \gamma' E$, where γ' is a constant. Repeating the above analysis, with the assumption that the form of the leading nonconstant term in the formal solution for $x(t)$ is $\sin \omega t$, leads to the result for the VACF,

$$\frac{\langle v(0)v(t)\rangle_{\text{can}}}{\langle v(0)^2\rangle_{\text{can}}} = \frac{\beta^2 \cos(\sqrt{2}t) + \gamma' \beta t \sin(\sqrt{2}t)}{\gamma'^2 t^2 + \beta^2}. \tag{27}$$

.

As shown below, this result agrees well with the numerical simulations.

B. Higher-order anharmonicity

We now outline the approach of Sarkar [10] in extracting the behavior of $\omega(E)$ for various potentials with leading anharmonic terms of the form x^{2n}, where $n>2$ and is an integer.

Starting with Eq. (12) and rewriting it as

$$\frac{\langle v(0)v(t)\rangle_{\text{can}}}{\langle v(0)^2\rangle_{\text{can}}} = \frac{\text{Re}\left(\int_0^\infty \exp^{-\beta E} \exp(\Phi(E)) it\omega(E) dE \right)}{\int_0^\infty \exp^{-\beta E} dE}, \tag{28}$$

we first assume, without any proof for now, that $\Phi(E)$ has an $(n-1)$th-order stationary point at $E=0$. This implies that all derivatives of $\omega(E)$ up to and including the $(n-2)$th order must vanish at $E=0$ but the $(n-1)$th-order derivative would be nonvanishing. We also note that the density of states, $g(E)$, goes to a nonzero constant as $E\to 0$. To see this behavior of $g(E)$ we note that the number of states $N(E)$ with energy up to E is proportional to the area in the x-p plane enclosed by the contour of energy E. As $E\to 0$, the motion becomes essentially harmonic and this area is proportional to E. Thus, $g(E) \equiv dN(E)/dE \to$ const.

If $\Phi(E)$ has an $(n-1)$th stationary point in E, then

$$\frac{\langle v(0)v(t)\rangle_{\text{can}}}{\langle v(0)^2\rangle_{\text{can}}} \propto \text{Re}[\exp(it\Phi(0)) + i\pi/2q]$$

$$\times [q!/t|\Phi^{\{(q)\}}(0)|]^{1/q} \Gamma(1/q)/q, \tag{29}$$

where $q=(n-1)$ and $\Phi^{\{(q)\}}(0)$ is the qth derivative of Φ evaluated at $E=0$. This leads us to the following prediction for asymptotic relaxation as $t\to\infty$:

$$\frac{\langle v(0)v(t)\rangle_{\text{can}}}{\langle v(0)^2\rangle_{\text{can}}} \propto \cos[\omega(0)t + \pi/2(n-1)]/t^{1/(n-1)}. \tag{30}$$

As we shall see later, our numerical analyses are consistent with the asymptotic behavior predicted by the analyses below.

The assumption regarding the $(n-1)$th-order stationary point in $\omega(E)$ made above can be justified as follows. We first observe that $\omega(E) = dJ(E)/dE$, where $J(E)$, the action, is by definition $\oint p(x)dx$, where $p(x)$ is the momentum of the particle as a function of its position. To establish that $\omega(E) \sim \omega(0) + \kappa E^{n-1}$, where κ is some constant, we must show that $J(E) = \alpha_1 E + \alpha_2 E^n + \cdots$, where α_1 and α_2 are appropriate constants.

Since $J(E)=\oint p(x)dx$ and is symmetric about $x=0$, one can write

$$J(E)=4\int_0^{U(E)}\sqrt{2\left(E-\frac{x^2}{2}-\frac{x^{2n}}{2n}\right)}dx, \tag{31}$$

where $U(E)$ is the right turning point. For a harmonic potential, $U(E)\equiv U_0(E)=\sqrt{2E}$. This implies that for the harmonic case $J(E)\equiv J_0(E)=\alpha_1 E$ and that in general, $J(E)=J_0(E)+\delta J(E)$. Thus, we need to establish that the leading term in $\delta J(E)\equiv\int_0^{U_0(E)}\sqrt{E-(x^2/2)}dx-\int_0^{U(E)}\sqrt{E-x^2/2-(x^{2n}/2n)}dx$ of the order E^n. Observe here that for $n>2$, $U_0(E)>U(E)$. As argued by Sarkar [10], one can write an expression for $\delta J(E)$ as follows:

$$\delta J(E)=\int_0^{U(E)}\sqrt{\left(E-\frac{x^2}{2}\right)}-\sqrt{E-\frac{x^2}{2}-\frac{x^{2n}}{2n}}dx+\int_{U(E)}^{U_0(E)}\sqrt{E-\frac{x^2}{2}}dx\equiv T_1(E)+T_2(E). \tag{32}$$

$U(E)$, which is the turning point of motion in the steeper potential, can be determined through perturbative techniques and is given by

$$U(E)=\sqrt{(2E)-\frac{(2E)^{2n-1/2}}{2n}+\frac{2n-1}{4n^2}(2E)^{2n-3/2}+\cdots}. \tag{33}$$

Using the expression for $U(E)$ above, one can show that $T_2(E)\sim E^{3n-1/2}$. To calculate $T_1(E)$, we observe that $\sqrt{E-x^2/2}-\sqrt{E-x^2/2-x^{2n}/2n}=[(x^{2n}/2n)/\sqrt{E-x^2/2}]f(x)$, where $f(x)=[1-\sqrt{1-y(x)}]/y(x)$ with $y(x)=(x^{2n}/2n)/E-x^2/2$. The range of x $[0,U(E)]$ maps onto the range $[0,1]$ for y and thus $f(x)$ is bounded above by 1 and below by σ with $1>\sigma>0$. The crucial point here is that σ is independent of E. Thus, $T_1(E)$ is bounded above and below by K and σK, respectively, where $K=\int_0^{U(E)}((x^{2n}/2n)/\sqrt{E-x^2/2})dx$. This integral turns out to be of order E^n. Since $T_1(E)$ is bounded from above and below by quantities of order E^n in the limit $E\to 0$, it must be of order E^n in this limit. Therefore, $T_2(E)\sim E^{2n-3/2}$ is dominated by $T_1(E)$, which is of order E^n as $E\to 0$ and hence $J(E)=\alpha_1 E+\alpha_2 E^n+\cdots$, which we set out to establish.

III. NUMERICAL METHOD

Here we describe the numerical method used to calculate the canonical ensemble autocorrelation functions. The key to the approach is the fact that at a fixed energy the autocorrelation functions are periodic with the same period τ as the motion of the particle in the Duffing potential. The microcanonical autocorrelation functions need only be calculated over one period of motion with the values at longer times given by $\langle v(0)v(t+\tau)\rangle=\langle v(0)v(t)\rangle$. The evaluation of the canonical autocorrelation function can be done in a straightforward manner by first evaluating the microcanonical autocorrelation functions at a number of discrete energies in the range $E_{\min}\leqslant E\leqslant E_{\max}$ and then performing the integration over dE.

The first step in the calculation of the microcanonical autocorrelation function is the determination of the period of motion for a given fixed energy. Particular care is taken at this stage since the accurate determination of the canonical autocorrelation function at long times depends crucially on the cancellation of a large number of terms of comparable magnitude but opposite sign. Small errors in the calculation of $\tau(E)$ can lead to large errors in the phase relations between different microcanonical ensembles at long times. A rough estimate of the period is obtained by integrating the classical equations of motion for a particle in the Duffing potential using a third-order Gear algorithm. The uncertainty in τ at this stage is given by $\delta\tau\equiv\delta t/n$, where δt is the integration time step and n is the number of periods of motion integrated over. The values $(\tau-\delta\tau)$ and $(\tau+\delta\tau)$ are then used as the bracketing values in a root finding routine which locates the zero of the function $f(\tau)=v(0)-v(\tau)$, where $v(\tau)$ is obtained by integrating the equations of motion using a time step $\delta t=\tau/1024$. This procedure is used to determine τ to a level of accuracy such that both $|x(0)-x(\tau)|$ and $|v(0)-v(\tau)|$ are less than 1×10^{-8}. Once a sufficiently accurate value of τ has been obtained, the functions $x(t)$, $v(t)$, and $a(t)$, and in turn, $\langle x(0)x(t)\rangle$, $\langle v(0)v(t)\rangle$, and $\langle a(0)a(t)\rangle$, are tabulated at 1024 equally spaced times spanning one period of motion. For the Duffing oscillator, the position, velocity, and acceleration autocorrelation functions should all be identical in the long-time limit, but they are evaluated as an additional test to make sure that the results of the calculation are consistent. The values of the microcanonical autocorrelation functions required in the integration are obtained via a linear interpolation between table entries.

The range of energies over which the microcanonical autocorrelation functions are calculated is determined by the temperature of the system. We choose as the lower limit of integration an energy slightly higher than the potential minimum, typically $E_{\min}=5\times 10^{-7}$, and, as the upper limit, $E_{\max}$ such that $\exp(-\beta E_{\max})$ is less than 1×10^{-11}. The canonical autocorrelation functions are evaluated using the microcanonical autocorrelation functions tabulated at up to 5000 distinct energies. For the Duffing well, fewer than 1000 energies are typically needed to obtain good results. Calculations involving the double well usually require a larger number of microcanonical function evaluations in order to accurately perform the integration over energies in the vicinity of the barrier height. The integration is carried out using a simple trapezoid rule. A higher-order integration scheme was not employed since we used an unequal energy spacing to maximize the number of function evaluations in the lower energy region. Calculations carried out using equally spaced energies show no significant deviation from those using unequal spacings. During the numerical integration, care is taken to minimize the effects of roundoff error by summing the contributions to the integral from highest to lowest energy.

IV. RESULTS OF NUMERICAL SIMULATIONS

In this section we compare the numerical and analytic results for the Duffing and double well oscillators with r set equal to 1. We can do this without any loss of generality since the same trends in the behavior of the canonical VACF

and corresponding power spectrum obtained for r will occur for different values of r, only at higher or lower temperatures. For these systems, the numerical and analytic results for the canonical VACF complement each other particularly well. The analytic form based on the lowest-order energy expansion of the formal solution agrees with the numerical result at all times for low temperatures ($\beta \geqslant 100$) and at long times for higher temperatures, but fails to describe the short-time behavior of the VACF at higher temperatures. This is due to the fact that the low-temperature limit of the analytic solution neglects contributions from terms involving higher powers of t^{-n}. The numerical approach, on the other hand, has been found to be most reliable at short times. For low temperatures, using fewer than 2000 energies, the Duffing well VACF's can be evaluated numerically for long times ($t \simeq 20\,000$) yielding results that agree with the asymptotic solution, while at higher temperatures spurious behavior of the VACF's begins at considerably shorter times.

A. Duffing oscillator

A comparison between the numerical and analytic results for the canonical VACF at $\beta = 100$ is shown in Figs. 1(a) and 1(b). The two sets of results agree to within roughly 1% over the entire range of times studied, with the largest relative errors occuring at shorter times. It should be noted that the difference between the analytic and numerical results is oscillatory, suggesting that even better agreement would be obtained by retaining higher-order terms in the expansion of the microcanonical VACF leading to additional corrections to the canonical VACF of the form $[\cos(t),\sin(t)]f(t)$.

For $\beta = 4$, Figs. 2(a) and 2(b) show that there is a significant deviation between the two results at short times, but that the analytic form matches the simulation almost exactly at times $t > 30$. The reader may observe that while Figs. 1(b) and 2(b) look identical at first sight, the magnitudes of the VACF at large times are much smaller in Fig. 2(b) when compared with the same in Fig. 1(b). This is expected in view of the fact that relaxation is expected to occur more rapidly at higher temperatures.

At much higher temperatures, the discrepancy between the analytic form and the numerical results becomes more dramatic. For $\beta = 0.01$, the analytic form bears virtually no resemblance to the numerical results at short times as evident in Figs. 3(a) and 3(b).

The power spectra of the VACF's are shown in Figs. 4–8 for β ranging from 100 to 0.01. At $\beta = 100.0$, the power spectrum consists of a single peak located at $\omega = 1.0$. As the temperature is increased, contributions from frequencies other than the harmonic frequency become increasingly important. At $\beta = 10.0$, the power spectrum has broadened significantly, most noticeably on the high-frequency side of the peak. Further increases in the temperature lead not only to a broadening of the power spectrum, but to the formation of a distinct broad peak with a maximum located above the harmonic frequency. At the highest temperatures, the power spectrum is clearly dominated by the broad peak, but the sharp peak at $\omega = 1.0$ is always present. Even at $\beta = 0.01$, a vestige of the harmonic peak persists.

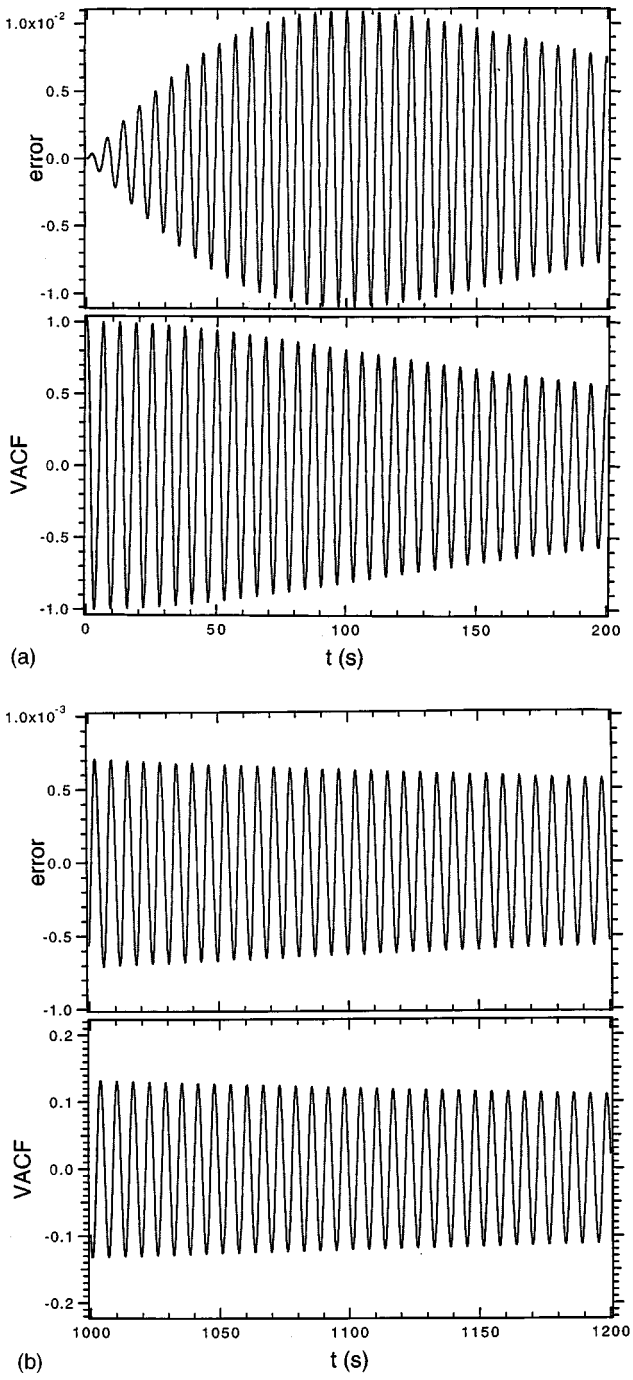

FIG. 1. Canonical ensemble VACF for Duffing well determined from numerical simulations and analytic form for $\beta = 100$ at times (a) $0 \leqslant t \leqslant 200$ and (b) $1000 \leqslant t \leqslant 1200$, where t is expressed in dimensionless form. The numerical and analytic results are indistinguishable in this plot. The upper panel displays the absolute difference, VACF (numerical) − VACF (analytic), between the two sets of results.

B. Double well oscillator

Figures 9–11 show a comparison between the numerical and analytic results for the double well at values of β equal to 100, 4, and 0.01. As was the case for the Duffing well, very good agreement is seen between the numerical and analytic results at low temperatures and long times. The oscillatory nature of the difference between the two sets of results

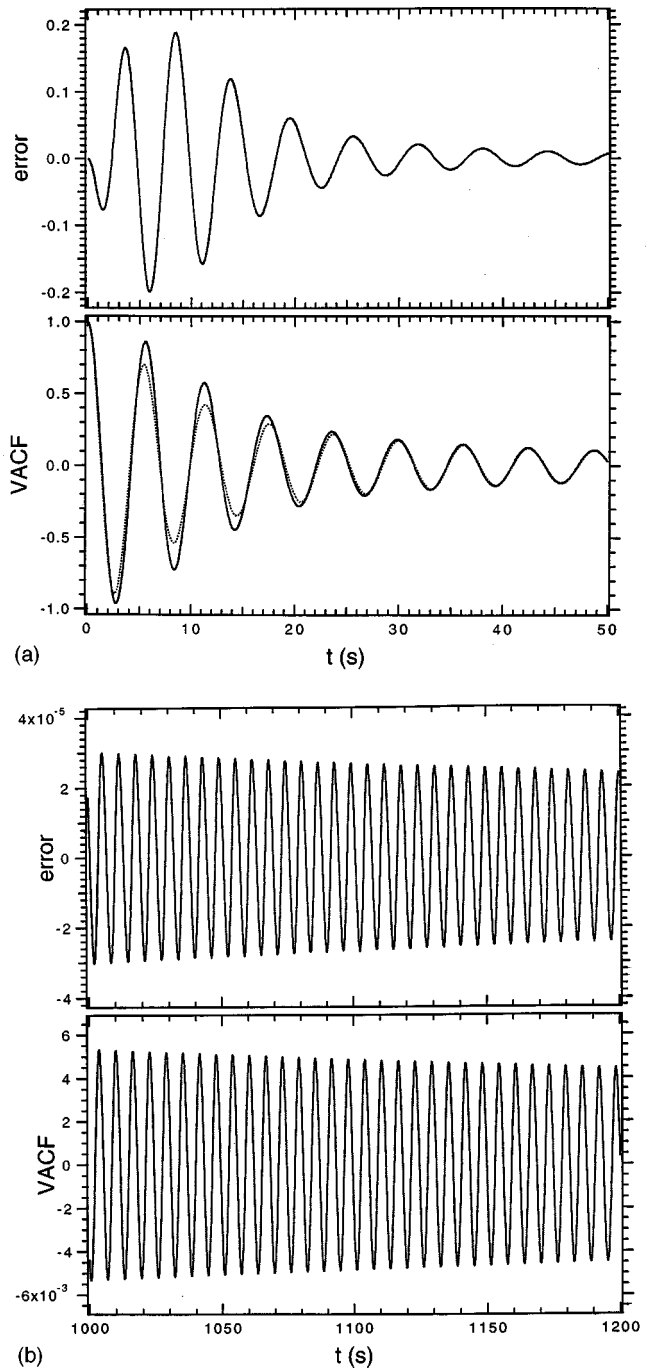

FIG. 2. Canonical ensemble VACF for Duffing well determined from numerical simulations (solid line) and analytic form (broken line) for $\beta=4$ at times (a) $0\leqslant t\leqslant 50$ and (b) $1000\leqslant t\leqslant 1200$, where t is expressed in dimensionless form. The upper panel displays the absolute difference, VACF (numerical)−VACF (analytic), between the two sets of results.

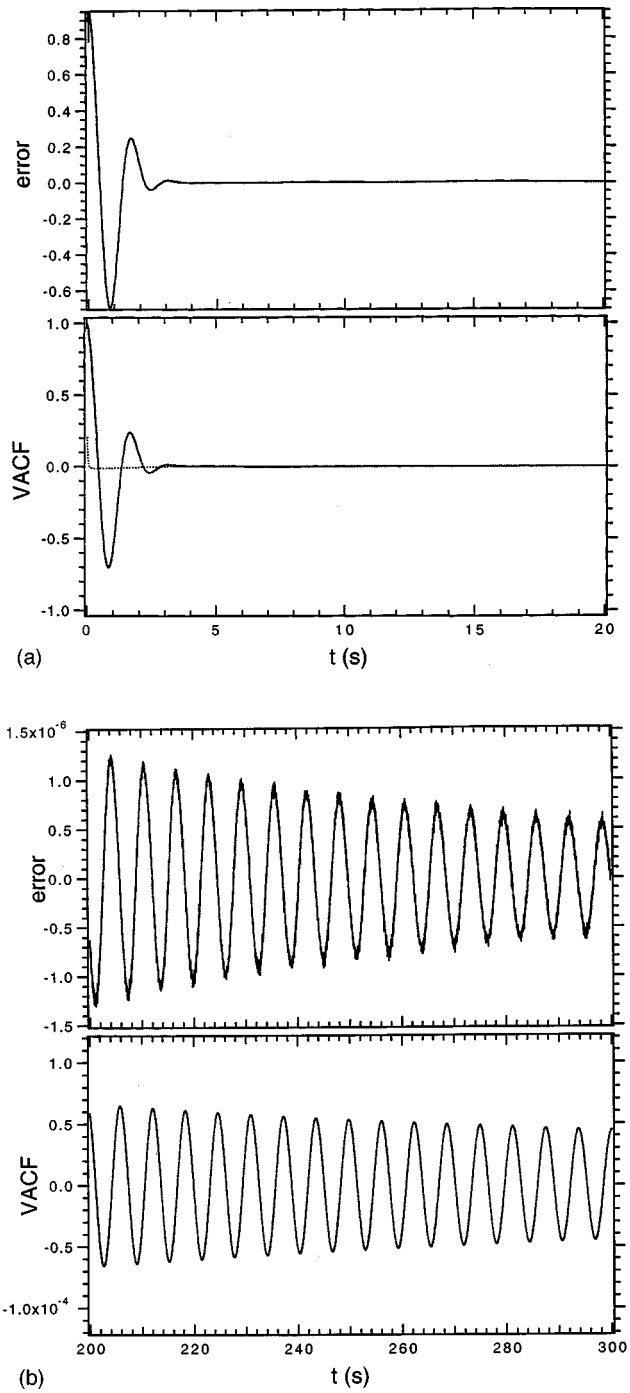

FIG. 3. Canonical ensemble VACF for Duffing well determined from numerical simulations (solid line) and analytic form (broken line) for $\beta=0.01$ at times (a) $0\leqslant t\leqslant 20$ and (b) $200\leqslant t\leqslant 300$, where t is expressed in dimensionless form. The upper panel displays the absolute difference, VACF (numerical)−VACF (analytic), between the two sets of results.

again suggests that the error is due to the omission of higher-order terms in the expansion of the microcanoncial VACF's.

The power spectra of the VACF's are shown in Figs. 12–16 for β ranging from 100 to 0.01. A gradual transition is seen from a single sharp peak at the harmonic frequency $\omega=\sqrt{2}$ for low temperatures to a broad spectrum at higher temperatures. In contrast to the Duffing well, the broadening of the power spectrum begins predominantly on the low-frequency side of the harmonic peak. At the highest temperatures, a remnant of the contribution from the harmonic frequency is still visible, but seems to manifest itself as a subtraction rather than an addition to the broadband.

It is important to state that we have found it somewhat difficult to explain the power spectra using intuitive arguments, e.g., in terms of the peak frequencies using Eqs. (3) and (7) in these systems at finite temperatures. However, this is not uncommon when analyzing strongly anharmonic sys-

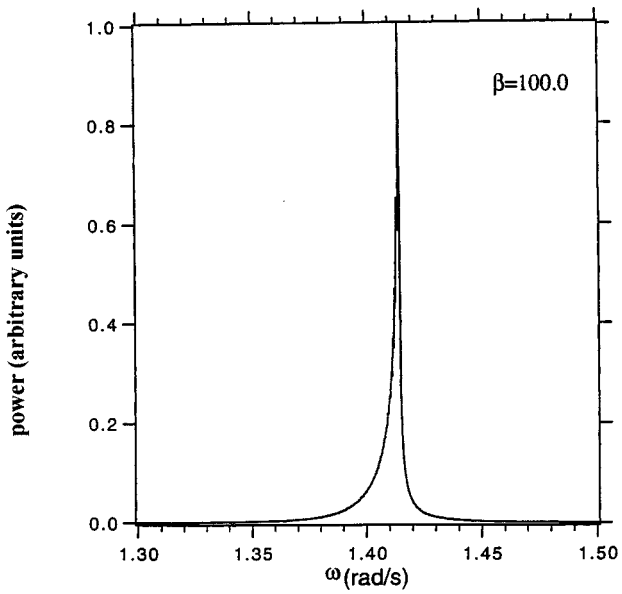

FIG. 4. Power spectrum of the Duffing well canonical VACF for $\beta=100$, where ω is expressed in dimensionless form.

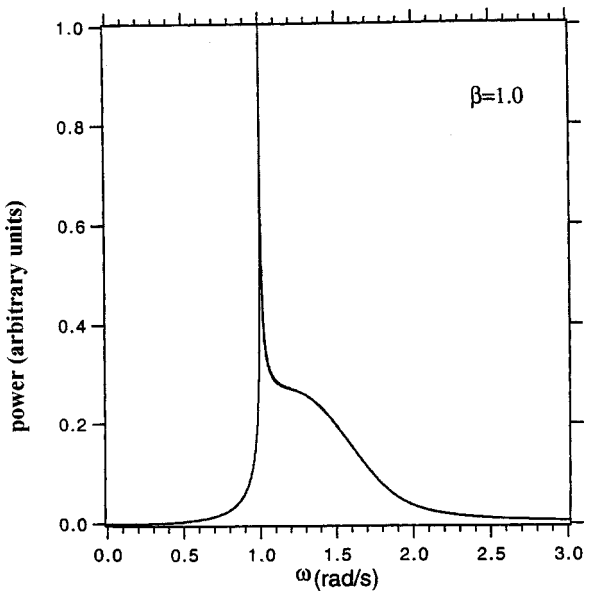

FIG. 6. Power spectrum of the Duffing well canonical VACF for $\beta=1$, where ω is expressed in dimensionless form.

tems, such as glasses and quantum spin systems at finite temperatures.

V. ARBITRARY ANHARMONICITY

We have extended our work to study the asymptotic behavior of the VACF in potentials of the form

$$V(x)=x^2/2+x^{2n}/2n, \tag{34}$$

where $n>2$. Typically, the calculations of long time behavior of the VACF get progressively more difficult with increasing n. As a consequence, it is a daunting task to numerically calculate the behavior of the algebraic tail in the VACF, which is of the form $1/t^{\phi}$, where $\phi<1$, at the asymptotic limit in time. Our calculated values of ϕ versus n are presented in Fig. 17. On the basis of these calculations, we predicted [7] that

$$\phi=1/(n-1). \tag{35}$$

As discussed in Sec. II B, Sarkar's method [10] arrives at the expression for ϕ given above and hence validates our claim. It remains difficult, however, to obtain the behavior of the VACF accurately at all time regimes in view of the steepness of the potential energy function and the strongly nonlinear dependence of $\omega(E)$ on E as discussed in Sec. II B.

Let us consider the potential function in Eq. (34) without the harmonic term and consider cases with extreme values of n. We note that the extreme limits of $n\rightarrow\infty$ and $n\rightarrow 1$ lead to

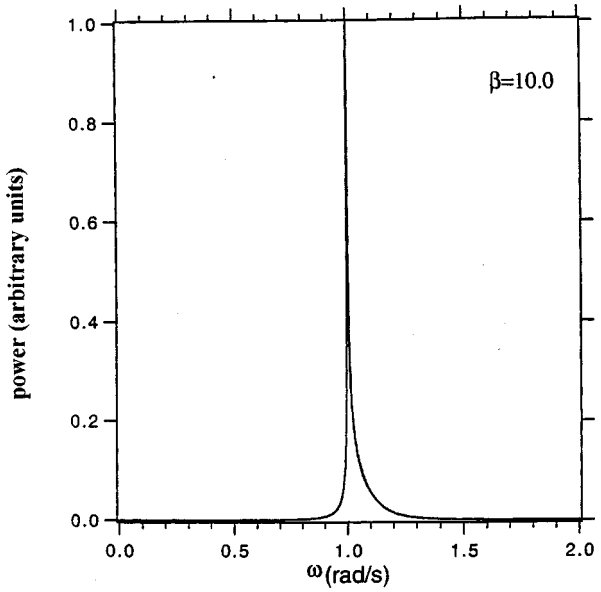

FIG. 5. Power spectrum of the Duffing well canonical VACF for $\beta=10$, where ω is expressed in dimensionless form.

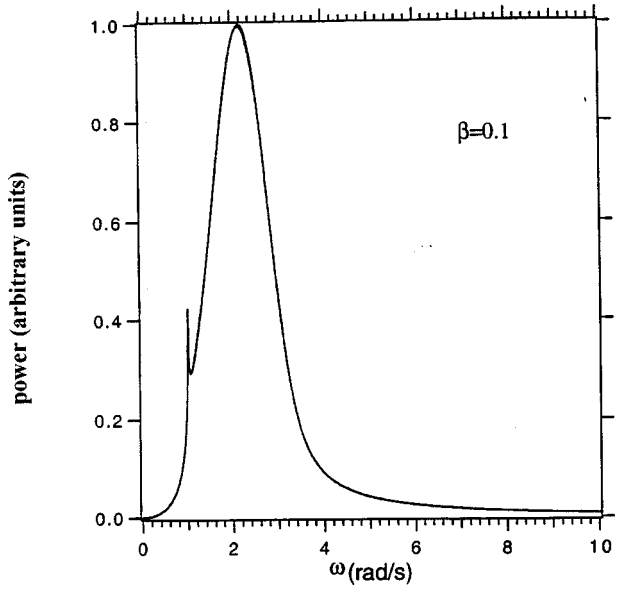

FIG. 7. Power spectrum of the Duffing well canonical VACF for $\beta=0.1$, where ω is expressed in dimensionless form.

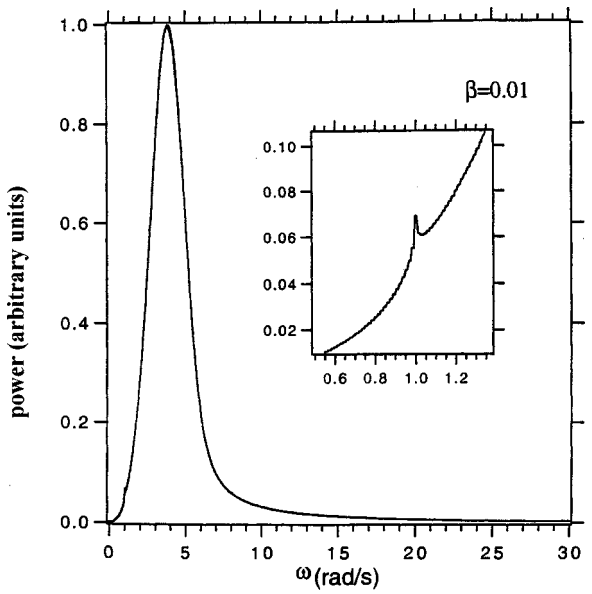

FIG. 8. Power spectrum of the Duffing well canonical VACF for $\beta=0.01$, where ω is expressed in dimensionless form. The inset shows the detail of the power spectrum in the vicinity of the harmonic frequency.

the following relaxation behavior. For $n\to\infty$, the anharmonicity in $V(x)$ becomes infinitely steep and $\omega(E)$ diverges to leading nonlinear order in E. This implies that $\phi\to 0$, or $1/t^{\phi}\to 1$. If the normalized VACF remains a constant in time, then the system exhibits no dynamics. To see the meaning of the preceding statement, we observe that for $n\to\infty$, the right-hand side of the equation of motion becomes divergent, implying that acceleration must diverge for motion to occur. As one would then expect, in a potential that is infinitely steep, any motion costs a tremendous amount of energy and thus no time evolution is possible.

For $n\to 1$, Eq. (34) reveals that $V(x)$ is entirely harmonic and according to Eq. (35), $\phi\to\infty$. Thus the VACF does not decay asymptotically in time, as is indeed the case for relaxation of the form of $\cos(\omega t)$ in the harmonic potential case. It should be noted that the nondecaying VACF result is distinct from the case in which the VACF remains unity, indicating that there is no time evolution at all.

VI. CONTINUED FRACTION FORMALISM BASED ANALYSES

In this section we present a brief discussion which suggests that no time series based approach, no matter how extensive, can estimate the asymptotic behavior $1/t^{\phi}$ presented in Secs. II–V.

The discussion in this section centers upon our current understanding of the continued fraction formalism which grew out of the classic works of Mori [12], Dupuis [13], Zwanzig [14], Lee [15], Grigolini [16], and others [17]. In this formalism one constructs a complete orthogonal set of d time-independent basis vectors f_ν with d time-dependent coefficients $a_\nu(t)$ (which are later identified with various fundamental dynamical correlations) to describe a dynamical variable $A(t)$ as follows [15]:

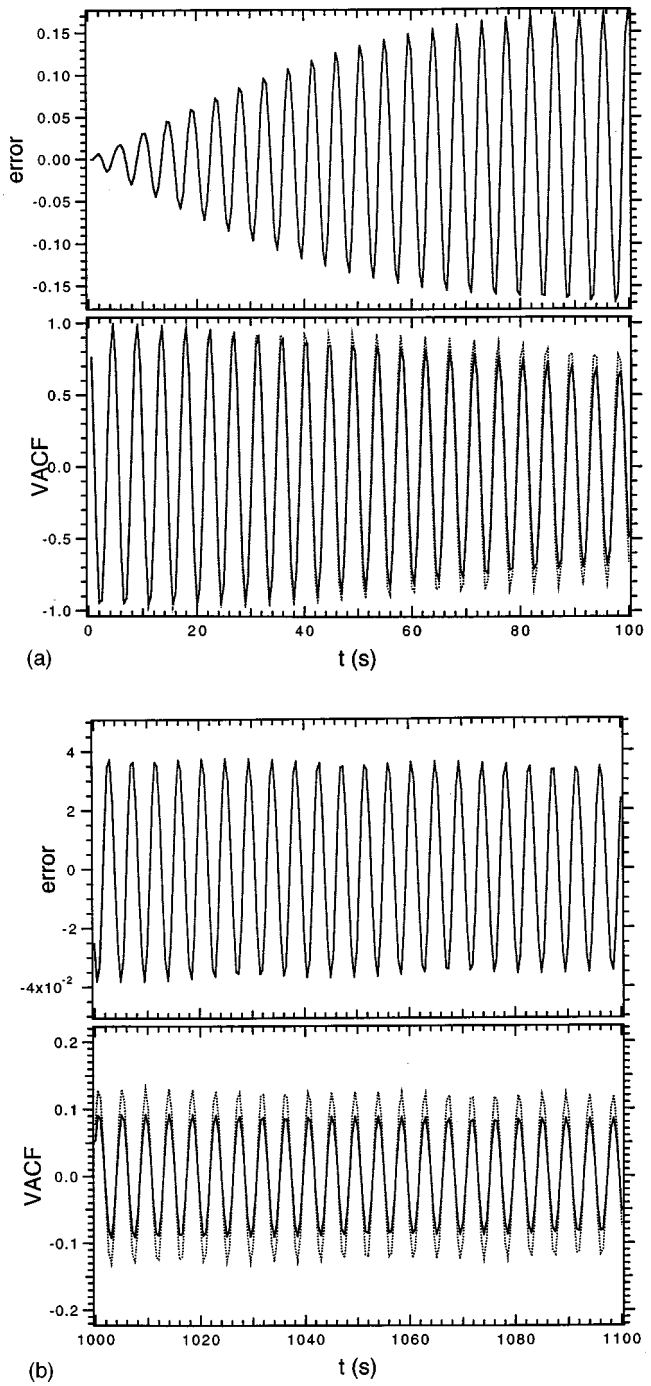

FIG. 9. Canonical ensemble VACF for double well determined from numerical simulations and analytic form for $\beta=100$ at times (a) $0\leqslant t\leqslant 100$ and (b) $1000\leqslant t\leqslant 1100$, where t is expressed in dimensionless form. The numerical and analytic results are indistinguishable in this plot. The upper panel displays the absolute difference, VACF (numerical) − VACF (analytic), between the two sets of results.

$$A(t)=\sum_{\nu=1}^{d-1} f_\nu a_\nu(t). \tag{36}$$

It is assumed that $A(t)$ satisfies the Liouville equation of motion [e.g., for the Hamiltonian in Eq. (4) this is Eq. (5)]. Typically, one *chooses* $f_0=A(t=0)$. The orthogonal f_ν's

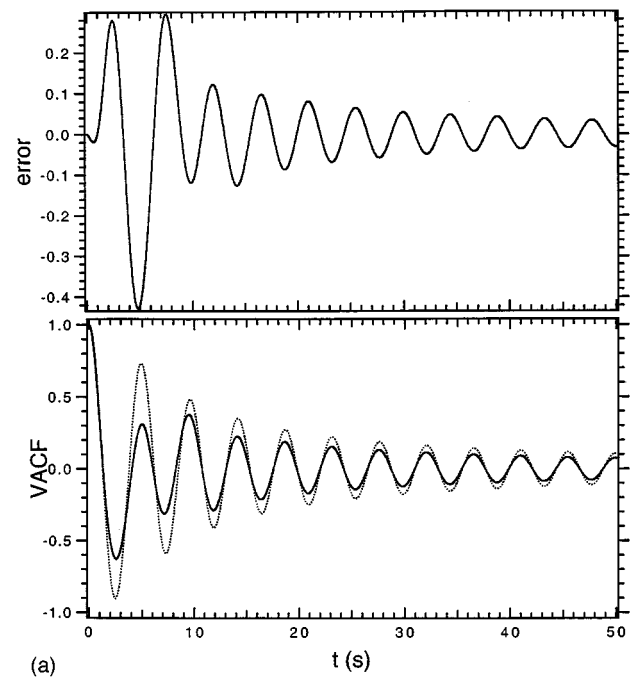

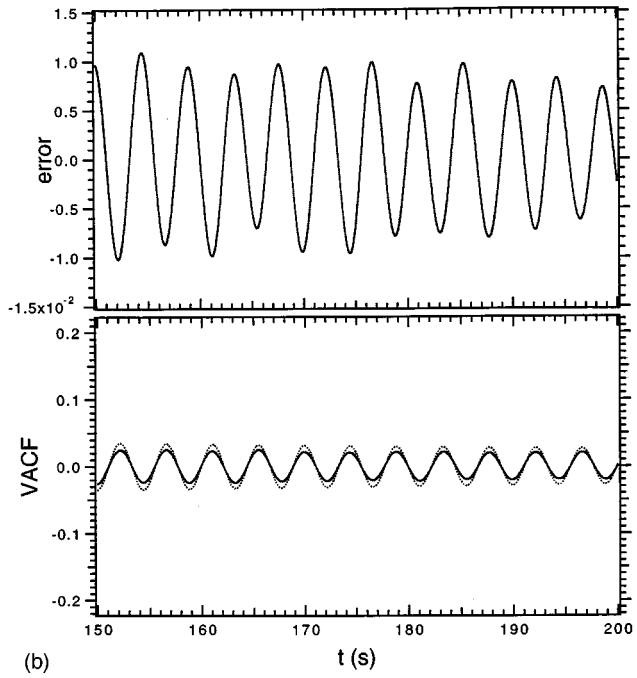

FIG. 10. Canonical ensemble VACF for double well determined from numerical simulations (solid line) and analytic form (broken line) for $\beta=4$ at times (a) $0\leqslant t\leqslant 50$ and (b) $150\leqslant t\leqslant 200$, where t is expressed in dimensionless form. The upper panel displays the absolute difference, VACF (numerical)$-$VACF (analytic), between the two sets of results.

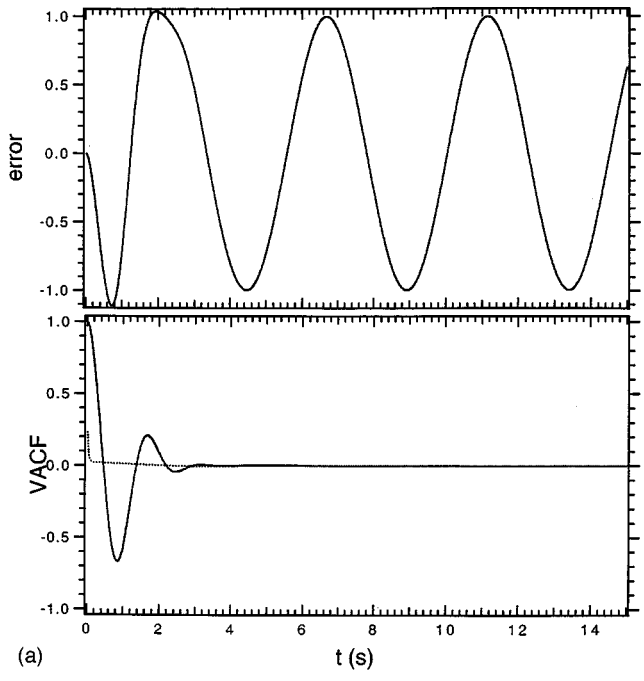

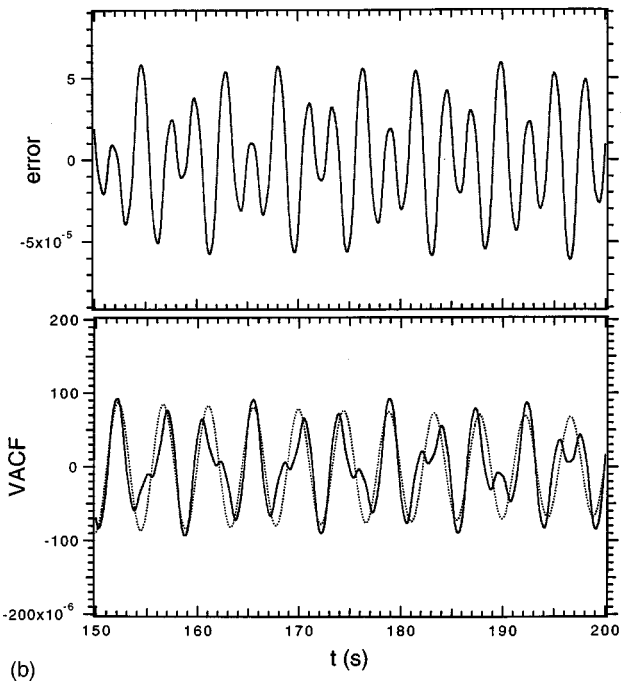

FIG. 11. Canonical ensemble VACF for double well determined from numerical simulations (solid line) and analytic form (broken line) for $\beta=0.01$ at times (a) $0\leqslant t\leqslant 15$ and (b) $150\leqslant t\leqslant 200$, where t is expressed in dimensionless form. The upper panel displays the absolute difference, VACF (numerical)$-$VACF (analytic), between the two sets of results.

can be suitably defined for a chosen problem. One typical choice for classical problems is the standard fluctuation formula, i.e.,

$$(X,Y)=\langle XY\rangle-\langle X\rangle\langle Y\rangle. \tag{37}$$

The notation $\langle\ \rangle$ denotes a canonical ensemble average. The choice of such a scalar product results in parametrization of $\{f_\nu\}$ and $\{a_\nu\}$ in terms of β and is hence well suited for the study of dynamical correlations in the canonical ensemble [18]. Observe that the choice of f_0 and that of the scalar product for imposing orthogonality of f_ν's imply that

$$a_0(t)=\frac{\langle A(t)A(0)\rangle}{\langle A(0)^2\rangle}, \tag{38}$$

which is the fundamental relaxation function for $A(t)$, the

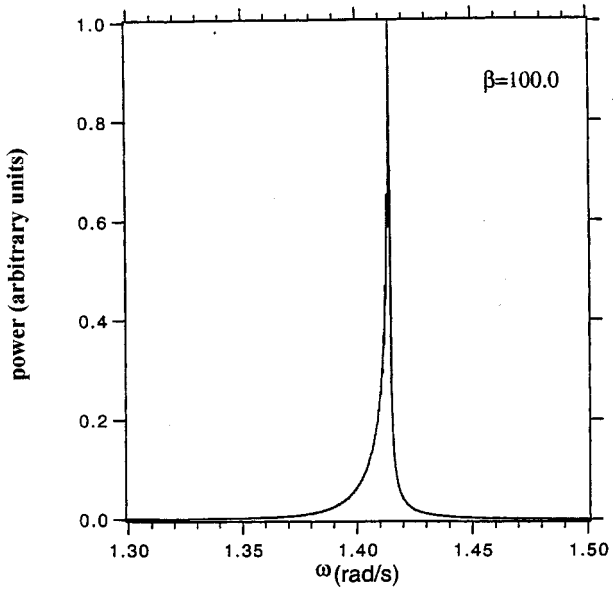

FIG. 12. Power spectrum of the double well canonical VACF for $\beta=100$, where ω is expressed in dimensionless form.

dynamical variable of interest. The f_ν's are constructed via a recurrence relation (RR I) [12–16],

$$f_{\nu+1}=Lf_\nu+\Delta_\nu f_{\nu-1}, \tag{39}$$

L above being the Liouville operator

$$Lf_\nu\equiv\sum_{i=1}^{N}\left(\frac{\partial f_\nu}{\partial x_i}\frac{\partial H}{\partial p_i}-\frac{\partial f_\nu}{\partial p_i}\frac{\partial H}{\partial x_i}\right) \tag{40}$$

for a classical system, and $\Delta_\nu\equiv(f_\nu,f_\nu)/(f_{\nu-1},f_{\nu-1})$, which are functions of equilibrium correlations of the system under study. The dynamical correlations are obtained by solving

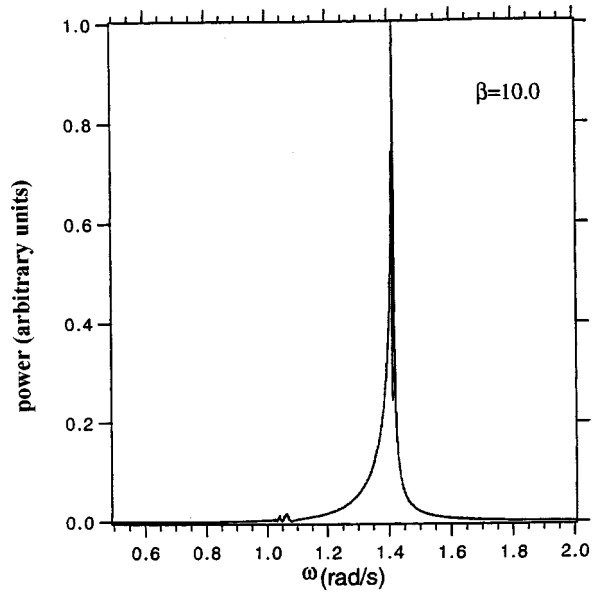

FIG. 13. Power spectrum of the double well canonical VACF for $\beta=10$, where ω is expressed in dimensionless form.

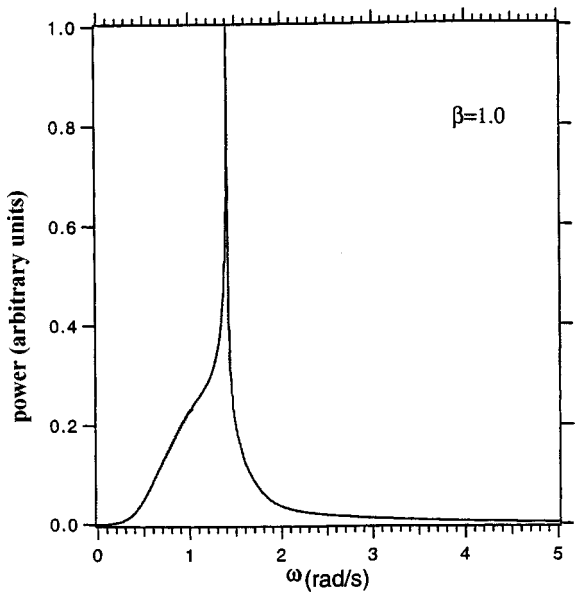

FIG. 14. Power spectrum of the double well canonical VACF for $\beta=1$, where ω is expressed in dimensionless form.

the Liouville equation for $A(t)$ with the chosen f_ν's, thereby satisfying a second recurrence relation (RR II) [15,16],

$$\Delta_{\nu+1}a_{\nu+1}(t)=-\dot{a}_\nu(t)+a_{\nu-1}(t). \tag{41}$$

RR II can be Laplace transformed and written as a continued fraction as follows [15,16]:

$$a_0(z)=1/(z+\Delta_1/\{z+\Delta_2/[z+\cdots\ \text{to}\ (d-1)]\}), \tag{42}$$

d being ∞ for ergodic systems [19–21]. Thus, if $a_0(z)$ which is a function of $\{\Delta_\nu\}$, $1\leqslant\nu<\infty$, which are functions of static correlations of the system described by the Hamiltonian H. If $\{\Delta_\nu\}$ is known, then in principle $a_0(z)$ can be obtained which upon inverse Laplace transformation then yields

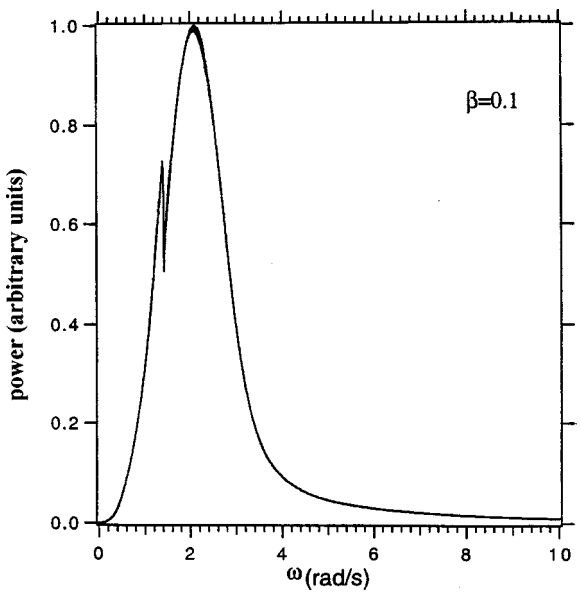

FIG. 15. Power spectrum of the double well canonical VACF for $\beta=0.1$, where ω is expressed in dimensionless form.

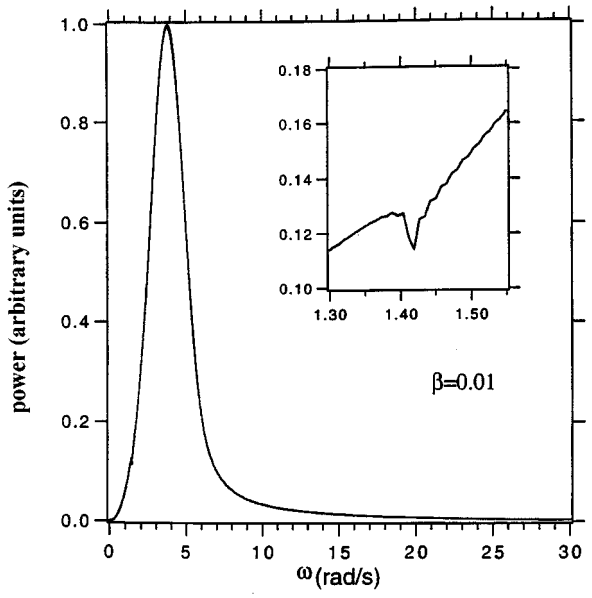

FIG. 16. Power spectrum of the double well canonical VACF for $\beta=0.01$, where ω is expressed in dimensionless form. The inset shows the detail of the power spectrum in the vicinity of the harmonic frequency.

$a_0(t)$, i.e., the relaxation function of interest. Once $a_0(t)$ is known, RR II allows one to readily obtain all $a_\nu(t)$'s. Complete knowledge of $\{f_\nu\}$ and $\{a_\nu(t)\}$ therefore solves for $A(t)$ [21].

For the Hamiltonian in Eqs. (1) and (2), if we set $A_i=B_i=C_i=0$ and $k_{i,i+1}=k$, and $A(t)=v_j(t)$, where v_j refers to the velocity of some tagged particle j in this translationally invariant system, then it can be shown that at all temperatures [22]

$$\Delta_1^{\rm hoc}=\frac{2k}{m},\quad \Delta_\nu^{\rm hoc}=\frac{k}{m},\quad \nu\geqslant 2, \tag{43}$$

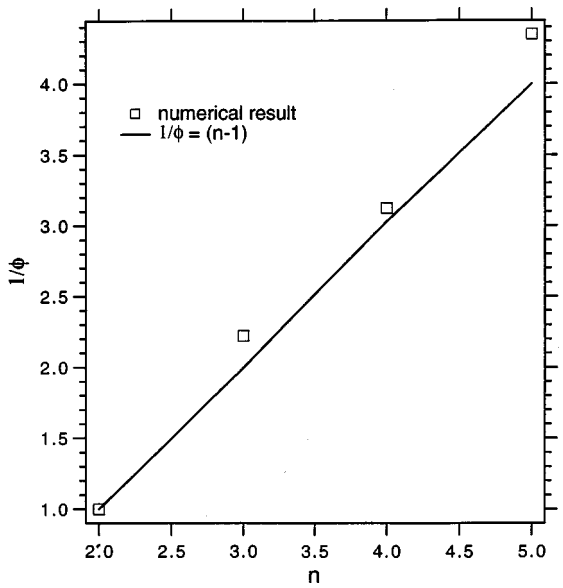

FIG. 17. Plot of $1/\phi$ versus n. ϕ is the relaxation exponent of any autocorrelation function which decays as $t^{-\phi}$ and n is the measure of leading anharmonicity.

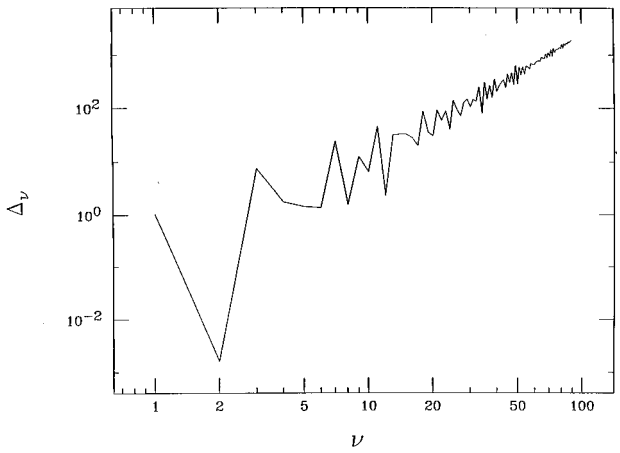

FIG. 18. Δ_ν versus ν for $n=2$ case calculated at $\beta=100$. The plot shows the emergence of scaling behavior for large ν.

i.e., as $\nu\to\infty$, $\Delta_\nu^{\rm hoc}\sim\nu^0$, where ''hoc'' refers to the harmonic oscillator chain. The physical meaning associated with this structure of Δ_ν's is described in detail in the latest article in Ref. [20] and in [23] and can be associated in real space in a linear harmonic chain with a linearly forward propagating excitation with respect to a point in space where an infinitesimal perturbation has been imparted.

However, if we set $k=0$, $n=2$, and $A_i\neq 0$, $B_i\neq 0$, and $C_i=0$ or $C_i\neq 0$, then the existing studies using a large but finite number of Δ_ν's (typically with $0<\nu\leqslant 100$) of Sen and Phillips and of Grossmann and Sonneborn-Schmick and of Fronzoni *et al.* among others suggest that at all finite temperatures as $\nu\to\infty$ [18,19,24]

$$\Delta_\nu\sim\nu^{2.5}. \tag{44}$$

Keeping in mind that in the absence of an exact solution this power-law growth is the best available estimate, one can say the Δ_ν's grow overwhelmingly fast compared to the growth in the case of the harmonic-oscillator chain [22,23]. Results of our calculation of Δ_ν for $n=2$ at $\beta=100$ are shown in Fig. 18.

We have recently computed the first 20 or so Δ_ν's for particles in potentials of the form $V(x)=x^2/2+x^{2n}/2n$, for $n=3$, 4, and 5. In all of these cases, we encountered difficulties in computing high-order Δ_ν's unless we restricted ourselves to extremely large values of β or low values of temperature. In spite of considering large β, eventually, typically for $\nu>25$ or so we found that the magnitudes of the Δ_ν's became large and unweildy. Based upon our calculations at $\beta=4$, we estimated $\chi_{n=3}\approx 2.7$, $\chi_{n=4}\approx 2.7$, and $\chi_{n=5}\approx 2.9$. We suspect that these previously unpublished values of χ are rough estimates for the actual growth rates in the Δ_ν's.

We are unable to obtain reliable information about the behavior of the VACF for $n=2$, 3, 4, and 5 using the continued fraction formalism approach. While this failure does not mean that the continued fraction formalism has inherent flaws, it does clearly reiterate an issue we have noted in earlier work [21], i.e., that continued fractions in which the $\Delta_\nu\sim\nu^\chi$ grow faster than $\chi=2$ cannot be replaced by finite continued fractions with an arbitrarily large number of levels, however large the number of levels may be. The problem

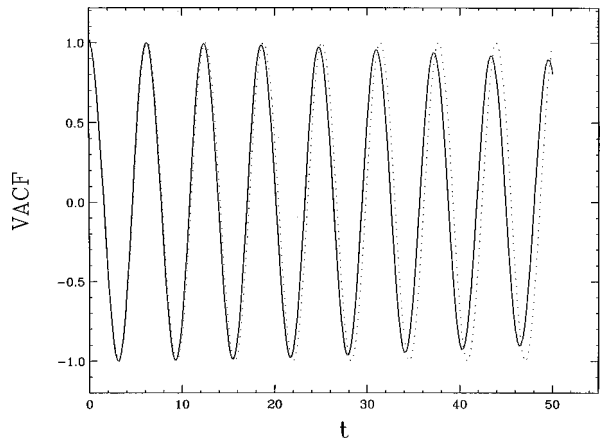

FIG. 19. Canonical ensemble VACF for $n=2$ (solid) and $n=3$ (dotted) cases showing different relaxation behavior but unable to capture the correct long-time tails. Time t is expressed as a dimensionless quantity. The calculations have been done using the calculated Δ_ν's and by truncating the continued fractions.

here is clearly analogous to what one encounters, for example, in calculating the free energy in the vicinity of a critical point in a system which is undergoing a phase transition by calculating the free energy using high- or low-temperature series expansion based approaches. Our calculations of the VACF for time $0 \leqslant t \leqslant 50$ for $n=2$ (solid) and 3 (dotted) are shown in Figure 19. Figure 20 shows the same calculations for $n=4$ (upper panel) and $n=5$ (lower panel). While it is obvious that the $n=3$ case exhibits slower relaxation than the $n=2$ case, the calculations do not capture the long time tails correctly. We see no difference between the VACFs in the $n=4$ and $n=5$ cases in Fig. 20, thereby indicating that the predicted VACFs using the direct summation approach are unreliable.

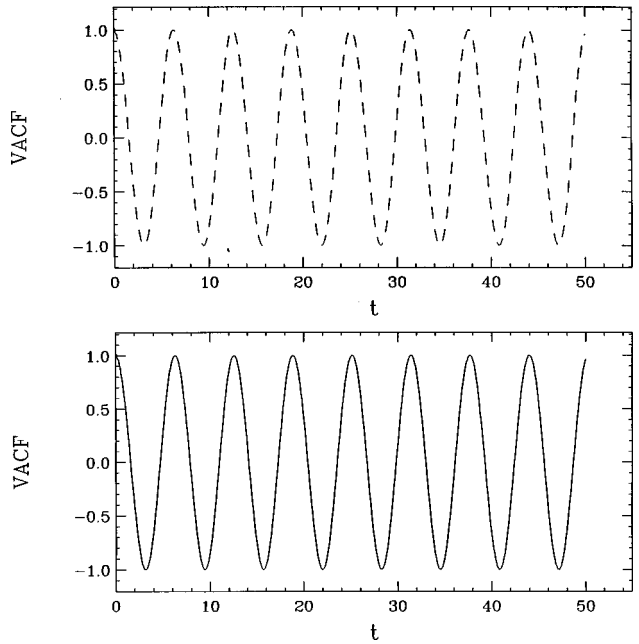

FIG. 20. Canonical ensemble VACF for $n=4$ (upper panel) and $n=5$ (lower panel) cases showing identical relaxation behavior but unable to capture the correct long-time tails. Time t is expressed as a dimensionless quantity. The calculations have been done using the calculated Δ_ν's and by truncating the continued fractions.

As shown in earlier work [21], the sequence of Δ_ν's for small ν and the asymptotic behavior of Δ_ν's jointly determine the relaxation properties under study. The former is easier to find than the latter. While we cannot directly estimate the continued fractions for $n=3,4,5$ cases using any known method, from the analyses presented in Secs. II and V, we know that the asymptotic relaxations differ in each of these cases according to the formula $1/t^\phi$, where $\phi=1/(n-1)$ (Fig. 17). Clearly, significant progress must be made in our understanding of the behavior of continued fractions for $\chi>2$. We are hopeful that the results on Δ_ν for $n\geqslant 2$ cases and the independent calculations of the relaxation behavior of these oscillators at all times will stimulate further investigations into approximating nonconvergent infinite continued fractions.

VII. APPLICATION TO MANY-BODY SYSTEMS

It is now known that anharmonic oscillators [18,24], small clusters [24], and similar few-body systems often exhibit high values of χ (i.e., $\chi>2$). Studies of many-body systems in finite lattice dimensions appear to show that the nature of propagation of an excitation in real space is intrinsically different when compared to the way in which the energy in a small perturbation distributes itself among the infinitely many frequencies of an anharmonic oscillator or an anharmonically coupled few-body system. However, the precise origins of the high values of χ as $\nu\rightarrow\infty$ remain to be understood or interpreted. Such an understanding is likely to help identify other physical systems in the same restricted dynamical universality class [20], i.e., with the same χ as $\nu\rightarrow\infty$.

Is it possible to estimate the growth rate of Δ_ν for the general problem posed in Eqs. (1) and (2) in which none of the relevant couplings vanish? The answer is yes but this is a daunting task which remains to be successfully carried out. Let us, however, explore some general features of what the solution to the complete problem described by Eqs. (1) and (2) must possess based upon what we already know about the structure of the f_ν's (and hence of the Δ_ν's) in Eq. (36). We first note that for the complete problem one can always separate the contributions to f_ν from $H_i^{\text{on-site}}$ and $H_{i,i+1}^{\text{int}}$ and the coupling of the anharmonic oscillator dynamics and the harmonic motion due to the two-body interactions. Hence one can express the terms arising from the harmonic springs and the anharmonic on-site potentials as f_ν^d (d refers to direct terms) and the terms arising from the coupling of the anharmonic potential and the harmonic springs as f_ν^c (c refers to cross terms) as follows:

$$f_\nu = f_\nu^d + f_\nu^c, \tag{45}$$

where to be more precise

$$f_\nu^d = f_\nu^{\text{hoc}} + f_\nu^{\text{anh}}; \quad f_\nu^c = f_\nu^{\text{hoc-anh}}. \tag{46}$$

In the above equation, f_ν^{hoc}, f_ν^{anh}, and $f_\nu^{\text{hoc-anh}}$ refer to the basis vectors for the harmonic-oscillator chain problem only, for the anharmonic potential problem only, and for the system in which the anharmonic potentials are coupled via harmonic springs, respectively. Indeed such arguments have

been used by Krumhansl and Schrieffer [1] more than twenty years ago when they treated the problem of dynamics of a one-dimensional system of particles in on-site double wells and connected by harmonic springs. The last basis vector is unknown for all ν at present. Clearly one can carry this logic a bit further and write the Δ_ν's in terms of direct and cross terms as follows:

$$\Delta_\nu = \Delta_\nu^d + \Delta_\nu^c, \tag{47}$$

where

$$\Delta_\nu^d = \Delta_\nu^d(\langle(f_\nu^{\text{hoc}})^2\rangle, \langle(f_\nu^{\text{anh}})^2\rangle) \tag{48}$$

and

$$\Delta_\nu^c = \Delta_\nu^c(\langle f_\nu^{\text{hoc}} f_\nu^{\text{anh}}\rangle, \langle f_\nu^{\text{hoc-anh}} f_\nu^{\text{hoc}}\rangle, \langle f_\nu^{\text{hoc-anh}} f_\nu^{\text{anh}}\rangle) \tag{49}$$

is an unknown part which remains to be determined. Since for k small compared to A_i, B_i, C_i (the order-disorder limit [1,8]), Δ_ν^c would become insignificant compared to Δ_ν^d, one would expect that

$$\Delta_\nu \approx \Delta_\nu^d \sim \nu^{2.5}. \tag{50}$$

The behavior of Δ_ν^c remains unknown for k strong.

If k is not overwhelmingly dominant compared to A_i, B_i, C_i, which determine the details of the anharmonic potential wells, then as $\nu \to \infty$, $\Delta_\nu \sim \nu^\chi$, where $\chi \geqslant 2.5$. This suggests that relaxation properties of such harmonically coupled particles in strongly anharmonic wells must be exceedingly slow, at least as slow as $1/t^\phi$, possibly even slower (the reader may recall that using existing methods, it is typically not possible to directly estimate the infinite continued fractions which have growth rates $\chi > 2.5$) [24].

VIII. CONCLUSION

In this paper we have presented the results of numerical simulations, together with analytic solutions, for the canonical VACF of the Duffing and double well oscillators and of oscillators described by potentials $V(x) = x^2/2 + x^{2n}/2n$ for $n = 3$, 4, and 5. The strong agreement between the analytic and numerical results, particularly at long times, gives us considerable confidence in the validity of the results. The analytic and numerical approaches complement each other particularly well for this problem since the numerical method is most reliable at short times, while an analytic form which describes the short-time, high-temperature regime quickly becomes unwieldy as higher-order terms in the expansion of the microcanonical VACF are retained.

The work described in this paper has led to some important new results regarding the Duffing and double well oscillators. First, we have analytically established that for the Duffing well, in the limit $t \to \infty$, the behavior of the VACF is given by $-(\beta/\gamma)\sin(t)/t$ at all temperatures. Numerical simulations are consistent with this asymptotic result. Second, a similar result, VACF $\sim (\beta/\gamma)\sin(\sqrt{2}t)/t$, has been obtained for the double well case. This finding has important implications for the relaxation of many physical systems. Third, we have demonstrated both via the asymptotic analyses of Sarkar [10] and via numerical calculations that for anharmonic potentials with $n > 2$, the algebraic tails of the asymptotic relaxation functions can be calculated and that they show reasonable agreement.

Finally, we have shown that for particles in anharmonic potentials the behavior of the Δ_ν's exhibits some of the fastest growth rates known to us. While we do not know how to estimate continued fractions with such rapid growth in Δ_ν's, we leave the reader with the eventual result one must reach by estimating these nonconvergent infinite continued fractions, namely, the finite and asymptotic time behavior of relaxation funtions for $n = 2$ and the asymptotic relaxation behavior for $n = 3$, 4, and 5 cases.

ACKNOWLEDGMENTS

We started our research on the problem discussed in this paper when Professor S.D. Mahanti posed certain questions regarding the relaxation of anharmonic oscillators to one of us (S.S.). Professor Daniel C. Mattis and Professor Paolo Grigolini encouraged us to attack this problem and pointed us toward some relevant literature. We are grateful to Professor Mahanti, Professor Mattis, and Professor Grigolini for drawing our attention to the problem of relaxation of anharmonic oscillators. We thank Professor Raj K. Pathria, Professor Subir K. Sarkar, Professor Deepak Dhar, Professor M. Howard Lee, and Professor Christopher Sorensen for valuable criticism at various stages of the work. S.S. acknowledges the efforts of Tony Ng, who meticulously checked the formulas reported in Ref. [11]. He also thanks Donald P. Visco, Jr. for sharing many insights into the dynamics in this problem. R.S.S. acknowledges the support of the U.S. Office of Naval Research through the U.S. Naval Research Laboratory, where most of his work was completed. S.S. was partially supported by the U.S. Army and by the U.S. Department of Energy through Sandia National Laboratories. J.C.P. was supported by the U.S. Department of Energy.

APPENDIX

Clearly, one's ability to calculate the infinite continued fraction in Eq. (42), which represents $a_0(z)$, rests upon one's success in calculating, or perhaps more importantly in estimating, the right-hand side of Eq. (42). Let us therefore comment on the behavior of Δ_ν below. The behavior of Δ_ν as a function of ν for small ν is typically very important in the description of the short time behavior and the long time behavior of the system under study. The asymptotic behavior of the relaxation process in time is, however, very sensitive to the manner in which Δ_ν behaves as $\nu \to \infty$ [21]. In the remainder of this paper our concern will center on the asymptotic behavior of Δ_ν.

One may begin by noting that any finite continued fraction contains a finite number of poles and hence a finite number of frequencies that characterize the dynamics. If any continued fraction truncates naturally, it must be for a system which shows nonergodic behavior in canonical ensembles [20,25]. Thus, if Δ_ν is an oscillatory or a decreasing function of ν, then the resulting continued fraction would lead to specific frequencies in the dynamics. Hence, for the relaxation function to go to zero as $t \to \infty$, Δ_ν must either be *independent* of ν or *grow* as a function of ν as $\nu \to \infty$. While we

cannot prove this statement analytically at this time, our numerical studies provide strong evidence in its support.

Some time ago, it was shown by direct numerical analysis that if as ν goes to ∞

$$\Delta_\nu \sim \nu^\chi, \tag{A1}$$

$\chi<2$, then Eq. (43) can always be numerically estimated by replacing Eq. (43) by a finite continued fraction which typically has 10^ζ levels, where typically $2\leqslant\zeta\leqslant5$ [21]. Upon a numerical inverse Laplace transform of Eq. (28) one then obtains $a_0(t)$ for $0\leqslant t\leqslant\rho$, where $\rho=f(\chi,\zeta)$ and is a large number, 10^η, $2\leqslant\eta\leqslant3$ being fairly typical numbers. If it so happens that the continued fraction is *convergent*, then a large enough ρ can always be found for an accurate estimation of the asymptotic relaxation properties.

Our numerical studies [21,26] show that it may happen that the continued fraction is *nonconvergent*, i.e., the Δ_ν's grow in such a way with ν that such continued fractions cannot be estimated by a finite number of poles no matter how large this number may be. For such continued fractions, for any $\zeta<\infty$, one cannot obtain any asymptotic features of the relaxation function $a_0(t)$ [24,27].

It turns out that for $\chi<2$, infinite continued fractions are *convergent* and hence *it is possible*, at least in principle, to obtain the asymptotic features of the relaxation function from careful numerical analysis of large but finite continued fractions along the lines indicated in Ref. [21]. However, for $\chi>2$, infinite continued fractions are *nonconvergent* and hence it *is not possible* to obtain the asymptotic features of the relaxation function from numerical analysis of large but finite continued fractions [21]. The case $\chi=2$ can be regarded as special. In a recent study, Lee *et al.* [28] have demonstrated a physical system exhibiting such behavior. The infinite continued fraction in this case is solvable analytically. Numerical studies in which the infinite continued fraction is replaced by a large but finite continued fraction do not readily yield the correct asymptotic behavior of the relaxation function (which turns out to be exponential decay) in this problem [21].

[1] J. Krumhansl and J.R. Schrieffer, Phys. Rev. B **11**, 3535 (1975).

[2] C. Dekker, A.F.M. Arts, H.W. de Wijn, A.J. van Duyneveldt, and J.A. Mydosh, Phys. Rev. B **40**, 11 243 (1989).

[3] S.Z. Ren and C.M. Sorensen, Phys. Rev. Lett. **70**, 1727 (1993); S. Z. Ren, W. F. Shi, W. B. Zhang, and C. M. Sorensen, Phys. Rev. A **45**, 2416 (1992).

[4] R.F. Fox, Phys. Rev. A **27**, 3216 (1983).

[5] J. Florencio, Jr. and M.H. Lee, Phys. Rev. A **31**, 3231 (1985).

[6] D. Vitali and P. Grigolini, Phys. Rev. A **39**, 1486 (1989).

[7] S. Sen, R.S. Sinkovits, and S. Chakravarti, Phys. Rev. Lett. **77**, 4855 (1996).

[8] A.D. Bruce and R.A. Cowley, *Structural Phase Transitions* (Taylor & Francis, London, 1981). In this connection see D.K. Chaturvedi and R. Singh, Phys. Rev. B **44**, 1193 (1991); S.D. Mahanti, H. Seong, S. Sen, and T. Cagin, Mol. Cryst. Liq. Cryst. Sci. Technol., Sect. A **245**, 141 (1994); H. Seong and S.D. Mahanti, Phys. Rev. B **49**, 5042 (1994).

[9] H.T. Davis, *Introduction to Nonlinear Differential and Integral Equations* (Dover, New York, 1962), p. 291.

[10] S.K. Sarkar, Phys. Rev. E **54**, 2465 (1996).

[11] J.P. Codaccioni and R. Caboz, J. Math. Phys. **25**, 2436 (1984).

[12] H. Mori, Prog. Theor. Phys. **33**, 423 (1965); **34**, 399 (1965).

[13] M. Dupuis, Prog. Theor. Phys. **37**, 502 (1967).

[14] R. Zwanzig, in *Lectures in Theoretical Physics*, edited by W.E. Brittin, B.W. Downs, and J. Downs (Wiley-Interscience, New York, 1961), Vol. 3; Annu. Rev. Phys. Chem. **16**, 67 (1965); S. Nordholm and R. Zwanzig, J. Stat. Phys. **13**, 347 (1975).

[15] M.H. Lee, Phys. Rev. Lett. **49**, 1072 (1982); Phys. Rev. B **26**, 2547 (1982); J. Math. Phys. **24**, 2512 (1983); M.H. Lee, Comput. Phys. Commun. **53**, 147 (1989); J. Hong, J. Korean Phys. Soc. **20**, 174 (1987).

[16] P. Grigolini, J. Stat. Phys. **27**, 283 (1982); P. Grigolini, G. Grosso, G. Pastori Parravicini, and M. Sparpaglione, Phys. Rev. B **27**, 7342 (1983); M. Giordano, P. Grigolini, D. Leporini, and P. Marin, Phys. Rev. A **28**, 2474 (1983); M.W. Evans, P. Grigolini, and G. Pastori Parravicini, *Memory Function Approaches to Stochastic Problems in Condensed Matter* (Wiley-Interscience, New York, 1985).

[17] For a comprehensive review, see A.S.T. Pires, Helv. Phys. Acta **61**, 988 (1988).

[18] This issue is briefly discussed in S. Sen and J.C. Phillips, Physica A **216**, 271 (1995) and in J.C. Phillips, National Science Foundation–Research Excellence for Undergraduates (NSF-REU) Program Report, Michigan State University, 1992.

[19] S. Grossmann and B. Sonneborn-Schmick, Phys. Rev. A **25**, 2371 (1982); L. Fronzoni, P. Grigolini, R. Mannella, and B. Zambon, J. Stat. Phys. **41**, 553 (1985), and references therein.

[20] S. Sen, Physica A **186**, 285 (1992); Phys. Rev. B **53**, 5104 (1996). The latter reference discusses the notion of the dynamical universality class in some detail.

[21] The complete program for numerical calculations appropriate for handling unsolvable infinite continued fractions appears in Z.-X. Cai, S. Sen, and S.D. Mahanti, Phys. Rev. Lett. **68**, 1637 (1992); S. Sen, Z.-X. Cai, and S.D. Mahanti, *ibid.* **72**, 3287 (1994); S. Sen, Z.-X. Cai, and S.D. Mahanti, Phys. Rev. E **47**, 273 (1993). For some successful applications see S. Sen, A.K.B. Engebretson, V.L. Gates, and L.I. McCann, Phys. Rev. B **50**, R4244 (1994); S. Sen and M. Long, *ibid.* **46**, 14 617 (1992).

[22] M.H. Lee, J. Florencio, Jr., and J. Hong, J. Phys. A **22**, L331 (1989).

[23] S. Sen, Phys. Rev. B **44**, 7444 (1991); Physica A **186**, 285 (1992).

[24] S. Sen and J.C. Phillips, Phys. Rev. E **47**, 3152 (1993).

[25] S. Sen, Proc. R. Soc. London, Ser. A **441**, 169 (1993).

[26] J.C.P. and S.S. have tried to approximately obtain the velocity relaxation function from the infinite continued fraction with the Δ_ν of the form in Eq. (42). By replacing this nonconvergent infinite continued fraction with a finite one with 5×10^5 levels, we obtained a $1/t^2$ relaxation at the largest times we could study without falling victim to round-off errors

($\sim 10^2$). This result of course implies that we were not able to reach the asymptotic limit which should have given $1/t$ behavior and is typical of problems encountered when continued fractions with $\chi > 2$ are perturbatively estimated. Clearly, extracting the result in some other way than directly estimating the nonconvergent infinite continued fractions for χ significantly greater than 2 is the desirable way to handle these problems.

[27] See also H.S. Wall, *Analytic Theory of Continued Fractions* (Chelsea, New York, 1948).

[28] M.H. Lee, J. Kim, W. Cummings, and R. Dekeyser, J. Phys.: Condens. Matter **7**, 3187 (1995).